Local polariton states in impure ionic crystals

V. S. Podolsky, Lev I. Deych, and A. A. Lisyansky
Department of Physics, Queens College, CUNY, Flushing, New York 11367
(Received 28 July 1997)

We consider the dynamics of an ionic crystal with a single impurity in the vicinity of the polariton resonance. We show that if the polariton spectrum of the host crystal allows for a gap between polariton branches, the defect gives rise to local states with frequencies within the gap. Despite the atomic size of the impurity we find that the in-gap local states are predominated by long-wavelength polaritons. The properties of these states are shown to be different from the properties of the well-known vibrational local states. The difference is due to the singular behavior of the density of states of polaritons near the low-frequency boundary of the polariton gap. Assuming cubic symmetry of the defect site we consider a complete set of the local states arising near the bottom of the polariton gap. [S0163-1829(98)05909-8]

I. INTRODUCTION

The existence of local excitations caused by crystal defects is a well-known phenomenon in solid-state physics.[1,2] A single pointlike defect can give rise to new states localized in the vicinity of a defect with frequencies outside the bands of extended states of a host crystal. These states and their interaction with electromagnetic waves (IR absorption, Raman scattering) have been extensively studied since the early 1940's following the pioneering works of Lifshitz.[3–5] In all these studies the electromagnetic field was considered as an external field, which excites the vibrational states. The feedback effect of the vibrations upon the electromagnetic field was neglected. However, in ionic crystals in the region of frequencies close to the crossing point of phonon and photon dispersion curves one has to take this effect into account because the coupling between electromagnetic waves and vibrations becomes so strong that a different kind of excitation—polaritons—emerges. In this situation the analyses of local vibrations and their interaction with electromagnetic field has to be done more carefully with taking the polariton effects into account. Such a consideration was carried out in Ref. 7 where a new kind of local excitation was discovered. It was shown in Ref. 7 that if the polariton spectrum of a crystal exhibits a gap between polariton branches, where the density of states of a host material is equal to zero, a defect embedded in the crystal gives rise to local states with frequencies within the gap. These states are a mix of the electromagnetic field and excitations of a host material. Their properties appeared to be quite different from those of known local phonon states. Unlike pure phonon systems, in the case of isotropic materials there is no minimum critical value of the ''strength'' of the impurity for local polariton states to appear. This feature was shown to be caused by a negative dispersion of optical phonons resulting in a nonmonotonic dispersion of polaritons.

A general analysis made in Ref. 7 refers to arbitrary ''polarization waves.'' It is applicable to a variety of excitations, such as phonon-polaritons, exciton-polaritons, etc. Concerning a particular case of phonon polaritons the model of a dipole interaction between scalar electromagnetic and polarization waves, used in Ref. 7, needs to be extended to account for a vector nature of the excitations. Moreover, the analysis of nonisotope impurities, affecting the elastic bonds around a defect, is not consistent within the scalar model.

In the present paper we take into account the vector nature of electromagnetic waves interacting with vibrations in crystals with cubic symmetry. We assumed that an impurity atom in addition to having a different mass can locally change elastic constants. The anisotropy of the crystal is assumed to be weak and is neglected in the long-wavelength limit. We obtained two series of local states which differ in parity. In agreement with the results of Ref. 7, all these states appear first at the bottom of the polariton gap for infinitesimally small variations of impurity parameters. This is shown to be caused by a singularity of the density of states in the lower polariton band. This singularity also provides that the localization of transverse polaritons is most effective near the lower boundary of the gap. We show that the local polariton states, unlike usual transverse extended states are affected by the interaction with the longitudinal phonon modes. This interaction narrows the frequency range available for the local polariton states.

II. POLARITONS IN A PURE CRYSTAL: ISOTROPIC APPROXIMATION

We consider below a body-centered-cubic (bcc) dielectric crystal with two oppositely charged ions per each elementary cell. The interaction between ions is assumed to be a central one. Denoting masses of the positive and negative ions as m_+ and m_-, respectively, and their displacements as $\mathbf{U}_\pm(r)$, where $\mathbf{r}$ belongs to the positive or negative sublattice, we can write down the equations of stationary lattice vibrations coupled to a coherent electric field, $\mathbf{E}(\mathbf{r})$:

$$m_\pm \omega^2 \mathbf{U}_\pm(r) \pm q\mathbf{E}(\mathbf{r}) = -\sum_s \left[\sum_{\mathbf{R}_s} \mathbf{f}(\mathbf{r}\mathbf{R}_s) + \sum_{\mathbf{R}'_s} \mathbf{f}'(\mathbf{r}\mathbf{R}'_s) \right], \tag{1}$$

where q denotes an ion charge and ω is the frequency.

The right-hand side of Eq. (1) presents all elastic forces acting on the ion hosted at the site $\mathbf{r}$. Vectors $\mathbf{R}_s$ and $\mathbf{R}'_s$ denote radius vectors of neighboring ions in the s-shell

spheres of the original and alternative sublattice, respectively. In the case of a central interaction the elastic forces within one sublattice have the form:

$$\mathbf{f}(\mathbf{r}\mathbf{R}_s) = -\frac{\beta(R_s)}{R_s^2}\mathbf{R}_s\{\mathbf{R}_s\cdot[\mathbf{U}_\pm(\mathbf{r})-\mathbf{U}_\pm(\mathbf{r}+\mathbf{R}_s)]\} \quad (2)$$

and forces between ions from different sublattices are

$$\mathbf{f}'(\mathbf{r}\mathbf{R}_s') = -\frac{\beta'(R_s')}{R_s'^2}\mathbf{R}_s'\{\mathbf{R}_s'\cdot[\mathbf{U}_\pm(\mathbf{r})-\mathbf{U}_\mp(\mathbf{r}+\mathbf{R}_s')]\}, \quad (2')$$

where the elastic constants of intra- and intersublattice interaction, $\beta(R)$ and $\beta'(R')$, depend on a distance between ions only.

A coherent electric field induced by the ionic vibrations $\mathbf{E}(\mathbf{r})$ invokes an additional pair of equations:

$$\nabla\cdot\mathbf{E}(\mathbf{r}) = -4\pi q\sum_{\mathbf{l}}[\mathbf{U}_+(l)\cdot\nabla\delta(\mathbf{r}-\mathbf{l}) - \mathbf{U}_-(l+b)\cdot\nabla\delta(\mathbf{r}-\mathbf{l}-\mathbf{b})], \quad (3)$$

$$\nabla\times[\nabla\times\mathbf{E}(\mathbf{r})]+\frac{\omega^2}{c^2}\mathbf{E}(\mathbf{r}) = -\frac{4\pi q\omega^2}{c^2}\sum_{\mathbf{l}}[\mathbf{U}_+(l)\,\delta(\mathbf{r}-\mathbf{l}) - \mathbf{U}_-(l+b)\,\delta(\mathbf{r}-\mathbf{l}-\mathbf{b})], \quad (4)$$

where vectors $\mathbf{l}$ denote lattice vectors, $\mathbf{b}$ is the basis vector, and c is the speed of light.

The lattice normal modes arise as simultaneous solutions of Eqs. (1), (3), (4). Fourier transformation of this system gives the dynamic equations in the momentum representation:

$$\begin{pmatrix} \hat{\mathbf{D}}(\mathbf{k})+\hat{\mathbf{F}}(\mathbf{k})-\omega^2 m_+ & \hat{\mathbf{D}}'(\mathbf{k})-\hat{\mathbf{F}}(\mathbf{k}) \\ \hat{\mathbf{D}}'(\mathbf{k})-\hat{\mathbf{F}}(\mathbf{k}) & \hat{\mathbf{D}}(\mathbf{k})+\hat{\mathbf{F}}(\mathbf{k})-\omega^2 m_- \end{pmatrix}\begin{pmatrix}\mathbf{A}_+(k)\\ \mathbf{A}_-(k)\end{pmatrix} = 0. \quad (5)$$

Here $\mathbf{A}_\pm(\mathbf{k})$ denotes the Fourier amplitudes of the displacements, $\hat{\mathbf{D}}(\mathbf{k})$ is the dynamical matrix of the intrasublattice interaction

$$\hat{\mathbf{D}}(\mathbf{k}) = \sum_s \frac{\beta(R_s)}{R_s^2}\sum_{\mathbf{R}_s}\mathbf{R}_s\otimes\mathbf{R}_s(1-e^{i\mathbf{k}\cdot\mathbf{R}_s}) + \frac{\beta'(R_s')}{R_s'^2}\sum_{\mathbf{R}_s'}\mathbf{R}_s'\otimes\mathbf{R}_s', \quad (6)$$

and $\hat{\mathbf{D}}'(\mathbf{k})$ is the dynamical matrix of the intersublattice interaction

$$\hat{\mathbf{D}}'(\mathbf{k}) = -\sum_s \frac{\beta'(R_s')}{R_s'^2}\sum_{\mathbf{R}_s'}\mathbf{R}_{s'}'\otimes\mathbf{R}_s' e^{i\mathbf{k}\cdot\mathbf{R}_s'}, \quad (6')$$

where $\mathbf{R}\otimes\mathbf{R}$ denotes the direct products of two vectors.

The Fourier amplitudes of the field induced by the lattice vibrations can be expressed as $\mathbf{E} = -\hat{\mathbf{F}}(\mathbf{A}_+-\mathbf{A}_-)/q$, with operator $\hat{\mathbf{F}}$ defined as follows:

$$\hat{\mathbf{F}}(\mathbf{k},\omega) = \frac{4\pi q^2}{a^3}\cdot\frac{\omega^2\hat{\mathbf{I}}-\mathbf{c}^2\mathbf{k}\otimes\mathbf{k}}{\omega^2-c^2k^2} = \frac{4\pi q^2}{a^3}\left(\hat{\mathbf{P}}_\parallel+\frac{\omega^2}{\omega^2-c^2k^2}\hat{\mathbf{P}}_\perp\right), \quad (7)$$

where $\hat{\mathbf{I}}$ is the unit tensor, $\mathbf{P}_\parallel^{\alpha\beta} = k_\alpha k_\beta/k^2$ and $\mathbf{P}_\perp^{\alpha\beta} = \delta_{\alpha\beta} - k_\alpha k_\beta/k^2$ are the longitudinal and transverse projectors, respectively.

The dynamical matrices given by Eqs. (6), (6′) are of a general type and solutions of Eq. (5), in general, do not split into longitudinal and transverse modes. However, considering long-wave excitations in weakly anisotropic crystals, we can make use of the isotropic approximation for the dynamical matrices:

$$\hat{\mathbf{D}}(\mathbf{k}) = \gamma_\parallel(k)\hat{\mathbf{P}}_\parallel+\gamma_\perp(k)\hat{\mathbf{P}}_\perp, \quad (8)$$

$$\hat{\mathbf{D}}'(\mathbf{k}) = \gamma_\parallel'(k)\hat{\mathbf{P}}_\parallel+\gamma_\perp'(k)\hat{\mathbf{P}}_\perp, \quad (8')$$

where scalar functions, $\gamma_\sigma(k)$ and $\gamma_\sigma'(k)$, can be expressed in terms of frequencies of longitudinal and transverse phonons. In a crystal of cubic symmetry the dynamical matrices become trivial at the center of the Brillouin zone:

$$\hat{\mathbf{D}}(\mathbf{0}) = -\hat{\mathbf{D}}'(\mathbf{0}) = \sum_s\frac{\beta'(R_s')}{R_s'^2}\sum_{\mathbf{R}_s'}\mathbf{R}_s'\otimes R_s' = \frac{1}{3}\hat{\mathbf{I}}\sum_s\beta'(R_s')Z_s', \quad (9)$$

where Z_s' denotes a total number of ions in the s shell and we make use of the identity, $\Sigma_{\mathbf{R}_s'}\mathbf{R}_s'\otimes\mathbf{R}_s' = \hat{\mathbf{I}}Z_s'R_s'^2/3$, valid in crystals with cubic symmetry. Equation (9) sets a condition for parameters in Eqs. (8), so that all $\gamma_\sigma(0)$ and $-\gamma_\sigma'(0)$ are equal to a positive constant $\gamma = 1/3\Sigma_s\beta'(R_s')Z_s'$.

In the isotopic approximation all normal modes of a crystal become either longitudinal or transverse, $\mathbf{A}_\pm^{(\sigma)}(\mathbf{k}) = \mathbf{e}_\sigma(\mathbf{k})A_\pm^{(\sigma)}(\mathbf{k})$, where $\mathbf{e}_\sigma(\mathbf{k})$ are longitudinal or transverse unit polarization vectors, σ is a polarization index. Equations (5), (8) give the following relation between the Fourier amplitudes of displacements in different sublattices:

$$A_+^{(\sigma)} = \frac{f_\sigma-\gamma_\sigma'}{\gamma_\sigma+f_\sigma-\omega^2 m_+}A_-^{(\sigma)}. \quad (10)$$

For longitudinal modes $f_\parallel = 4\pi q^2/a^3 = f$. The corresponding dispersion equation,

$$\left(\frac{\gamma_\parallel+f_\parallel}{m_+}-\omega^2\right)\left(\frac{\gamma_\parallel+f_\parallel}{m_-}-\omega^2\right)-\frac{(\gamma_\parallel'-f_\parallel)^2}{m_+m_-} = (\omega^2-\omega_{+\parallel}^2)(\omega^2-\omega_{-\parallel}^2) = 0, \quad (11)$$

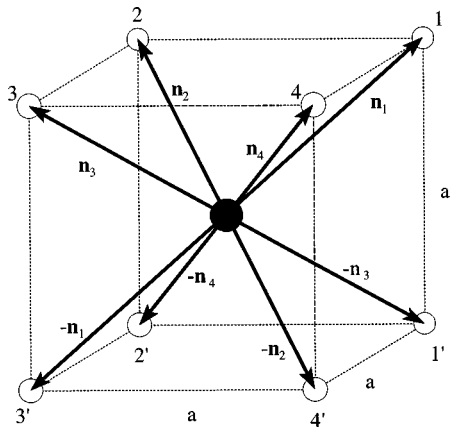

FIG. 1. Elementary cell of a body-centered-cubic lattice. Here a is a lattice parameter, indexes s,s' numerate ions within the near-neighbor shell, $\pm\mathbf{n}_s$ are radius vectors of the ions.

defines acoustic $\omega_{\parallel}^2(k)$ and optical $\Omega_{\parallel}^2(k)$ branches of longitudinal phonons. For transverse modes $f_{\perp}=f\omega^2/(\omega^2-c^2k^2)$, therefore, the dispersion equation,

$$\left(\frac{\gamma_{\perp}+f_{\perp}}{m_+}-\omega^2\right)\left(\frac{\gamma_{\perp}+f_{\perp}}{m_-}-\omega^2\right)-\frac{(\gamma'_{\perp}-f_{\perp})^2}{m_+m_-}$$
$$=\frac{(\omega^2-\omega_{\perp}^2)(\omega^2-\Omega_+^2)(\omega^2-\Omega_-^2)}{\omega^2-c^2k^2}=0, \qquad (12)$$

gives one acoustic $\omega_{\perp}^2(k)$ and two polariton $\Omega_{\pm}^2(k)$ branches.

Neglecting the field effects and solving Eqs. (11), (12) in the long-wavelength limit one can obtain expressions for $\gamma_{\sigma}(k)$ and $\gamma'_{\sigma}(k)$ in terms of conventional parameters:

$$\gamma_{\sigma}(k)\approx\gamma+\mu k^2(v_{\sigma}^2-v_{\sigma}'^2), \qquad (13)$$

$$\gamma'_{\sigma}(k)\approx-\gamma+\mu k^2\left[v_{\sigma}'^2+v_{\sigma}^2\left(\frac{M}{2\mu}-1\right)\right], \qquad (13')$$

where μ and M are reduced and total masses of ions within the elementary cell, respectively, v_{σ} and v'_{σ} are the velocities of acoustic and optical phonons with a given polarization.

Equations (11), (12) show that the internal field affects dispersion relations of all lattice excitations. However, the physical effects of the photon-phonon interaction are substantial in the vicinity of the polariton resonance which takes place in the long-wavelength region. It is straightforward to show that the acoustic branches,

$$\omega_{\sigma}^2(k)\approx 2\frac{\gamma_{\sigma}+\gamma'_{\sigma}}{M}\approx v_{\sigma}^2k^2, \qquad (14)$$

are unaffected by the field, whereas, the interaction with the field results in the uniform up-shift of the longitudinal-optical branch,

$$\omega^2=\Omega_{\parallel}^2(k)+d^2, \qquad (15)$$

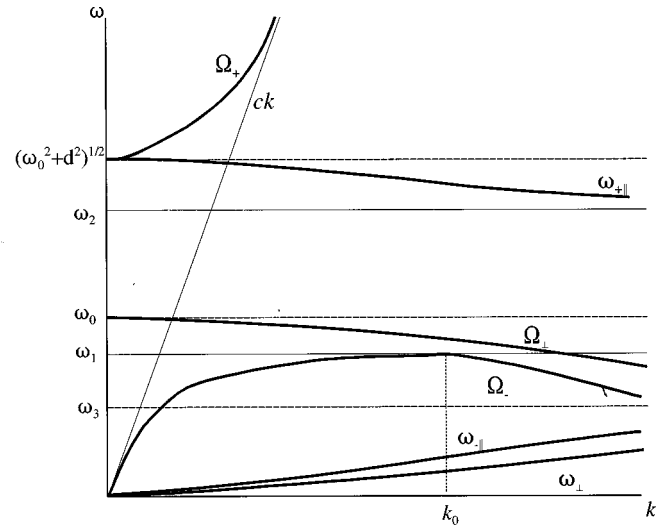

FIG. 2. Phonon-polariton dispersion curves in the isotropic approximation. Here lines $\omega=\Omega_{\pm}(k)$ present the lower and upper polariton branches, $\Omega_{\perp}(k)$ and $\omega_{+\parallel}(k)$ are transverse- and longitudinal-optical phonon branches, $\omega_{\perp}(k)$ and $\omega_{-\parallel}(k)$ are the transverse- and longitudinal-acoustic phonon branches, respectively. The horizontal lines ω_0 and ω_3 are the upper and lower boundaries of the transverse-optical phonon band, $\sqrt{\omega_0^2+d^2}$ and ω_2 are the upper and lower boundaries of the longitudinal-optical phonon band, respectively. The polariton gap is bounded by lines ω_1 and ω_2. The wave number k_0 corresponds to the maximum of the lower polariton branch. The figure presents qualitative features of phonon-polariton spectra in the long-wavelength region and does not reflect an actual scale of wave velocities.

and leads to the well-known polariton dispersion relation for optical-transverse excitations,[6,8]

$$[\omega^2-\Omega_{\perp}^2(k)][\omega^2-c^2k^2]=d^2\omega^2. \qquad (16)$$

Equation (16) describes two polariton branches $\Omega_{\pm}(k)$ with corresponding dispersion laws:

$$\Omega_{\pm}^2(k)=1/4\{\sqrt{[\Omega_{\perp}(k)+ck]^2+d^2}\pm\sqrt{[\Omega_{\perp}(k)-ck]^2+d^2}\}^2, \qquad (17)$$

where $\Omega_{\perp}$ and $\Omega_{\parallel}$ are frequencies of the transverse- and longitudinal-optical phonons, respectively,

$$\Omega_{\sigma}^2(k)\approx\frac{\gamma_{\sigma}}{\mu}-2\frac{\gamma_{\sigma}+\gamma'_{\sigma}}{M}\approx\omega_0^2-v_{\sigma}'^2k^2, \qquad (18)$$

a phonon-photon coupling parameter, $d^2=f/\mu=4\pi q^2/\mu a^3$, is the ionic ''plasma frequency'' and $\omega_0^2=\gamma/\mu$ is the optical activation frequency.

Analysis of Eqs. (14), (15), (17) shows that the lower polariton branch $\Omega_-^2(k)$ has a zero activation frequency and extends over both acoustic bands, whereas, the longitudinal-optical branch, $\Omega_{\parallel}^2(k)+d^2$, overlaps with the top part of the polariton gap. Therefore, a truly forbidden gap, with no modes of any kind inside, may exist only between the lower boundary of the polariton gap and the bottom of the longitudinal band (Fig. 1). When the dispersion of optical phonons

is neglected, both polariton branches are monotonic and the spectral gap is between the transverse and longitudinal frequencies, ω_0^2 and $\omega_0^2+d^2$.

It turns out that accounting for the phonon dispersion causes a *qualitative* change of this picture. First, the upper boundary of the frequency gap ω_2^2 is now set by the bottom of the optical-longitudinal band. Second, the lower polariton branch in the case of a negative dispersion becomes nonmonotonic and gains a maximum at some $k=k_0$, close to the center of the Brillouin zone (Fig. 1). Calculations in the long-wavelength approximation give $k_0^2 \approx 2\omega_0 d/v_\perp' c$ and a new lower boundary of the gap, $\omega_1^2=\Omega_-^2(k_0)\approx\omega_0^2 - 2v_\perp'\omega_0 d/c$. Since $2v_\perp'\omega_0 d/c \approx v_\perp'^2 k_0^2 \ll \omega_0^2$, the result is consistent with the approximation. However, because $c^2k_0^2 \approx 2c\omega_0 d/v_\perp' \gg \omega_0^2$, the maximum of $\Omega_-^2(k)$ is far away from the very narrow (due to $c \gg v_\perp'$) polariton resonance region. Since $\Omega_-^2(k)$ reaches its maximum at the surface of a finite area inside the Brillouin zone, the density of polariton states diverges at the gap's lower boundary. As we show later, it causes an absence of a lower threshold for local polariton states.

III. POLARITON LOCAL STATES

When a host ion at the site $\mathbf{r}=\mathbf{0}$ of the positive sublattice is replaced by an impurity ion with the same charge, it causes a local deviation of the crystal density and a local change of elastic constants. To account for these facts we need to add extra forces to the right-hand side of Eq. (1). For positive and negative sublattices, respectively, these forces are

$$\delta\mathbf{f}^+(r)=\left\{\omega^2\delta m\mathbf{U}_+(0)-\frac{\delta\beta}{n^2}\sum_{\mathbf{n}}\mathbf{n}[\mathbf{n}\cdot\mathbf{U}_+(\mathbf{0}) - n\cdot\mathbf{U}_-(\mathbf{n})]\right\}\delta_{\mathbf{r}\,\mathbf{0}} \tag{19}$$

and

$$\delta\mathbf{f}^-(r)=-\frac{\delta\beta}{n^2}\sum_{\mathbf{n}}\mathbf{n}[\mathbf{n}\cdot\mathbf{U}_+(\mathbf{0})-\mathbf{n}\cdot\mathbf{U}_-(\mathbf{n})]\delta_{\mathbf{r}\,\mathbf{n}}, \tag{19'}$$

where δm is the difference between the masses of an impurity and a host ion, $\delta\beta$ is a shift in the elastic constant in the impurity's near-neighbor shell, and vectors $\mathbf{n}$ denote radius vectors of the impurity's nearest neighbors.

The dynamic equation (5) is now modified:

$$\begin{pmatrix}\hat{\mathbf{D}}(\mathbf{k})+\hat{\mathbf{F}}(\mathbf{k})-\omega^2 m_+ & \hat{\mathbf{D}}(\mathbf{k})-\hat{\mathbf{F}}(\mathbf{k})\\ \hat{\mathbf{D}}(\mathbf{k})-\hat{\mathbf{F}}(\mathbf{k}) & \hat{\mathbf{D}}(\mathbf{k})+\hat{\mathbf{F}}(\mathbf{k})-\omega^2 m_-\end{pmatrix}\begin{pmatrix}\mathbf{A}_+(\mathbf{k})\\ \mathbf{A}_-(\mathbf{k})\end{pmatrix} = \frac{1}{N}\begin{pmatrix}\mathbf{B}_+\\ \mathbf{B}_-\end{pmatrix}, \tag{20}$$

where N is the number of ions in one sublattice and

$$\mathbf{B}_+=\omega^2\delta m\mathbf{U}_+-\frac{\delta\beta}{n^2}\sum_{\mathbf{n}}\mathbf{n}[\mathbf{n}\cdot\mathbf{U}_+-\mathbf{U}_{\mathbf{n}}], \tag{21}$$

$$\mathbf{B}_-=\frac{\delta\beta}{n^2}\sum_{\mathbf{n}}\mathbf{n}[\mathbf{n}\cdot\mathbf{U}_+-U_{\mathbf{n}}]e^{-i\mathbf{k}\cdot\mathbf{n}}. \tag{21'}$$

Here $\mathbf{U}_+=U_+(\mathbf{0})$ and all $\mathbf{U}_-(\mathbf{n})$ appear only in combinations $U_{\mathbf{n}}=\mathbf{n}\cdot\mathbf{U}_-(\mathbf{n})$, because ion-ion forces are central.

Let us denote the matrix in the left-hand side of Eq. (20) as $\mathbf{L}$. It acts on Cartesian (α) and sublattice (ε) indices of the amplitudes A_ε^α. In the isotropic approximation this matrix can be decomposed, $\mathbf{L}=\mathbf{L}_\parallel\otimes\hat{\mathbf{P}}_\parallel+\mathbf{L}_\perp\otimes\hat{\mathbf{P}}_\perp$, where 2×2 matrices $\mathbf{L}_\sigma$, operating on sublattice indexes only, are defined as follows:

$$\mathbf{L}_\sigma=\begin{pmatrix}l_\sigma^+ & l_\sigma'\\ l_\sigma' & l_\sigma^-\end{pmatrix}=\begin{pmatrix}\gamma_\sigma+f_\sigma-\omega^2 m_+ & \gamma_\sigma'-f_\sigma\\ \gamma_\sigma'-f_\sigma & \gamma_\sigma+f_\sigma-\omega^2 m_-\end{pmatrix}. \tag{22}$$

The inverse matrix, $\mathbf{L}^{-1}=\mathbf{L}_\parallel^{-1}\otimes\hat{\mathbf{P}}_\parallel+\mathbf{L}_\perp^{-1}\otimes\hat{\mathbf{P}}_\perp=\mathbf{G}=\mathbf{G}_\parallel\otimes\hat{\mathbf{P}}_\parallel + \mathbf{G}_\perp\otimes\hat{\mathbf{P}}_\perp$, where

$$\mathbf{G}_\sigma=\begin{pmatrix}g_\sigma^+ & g_\sigma'\\ g_\sigma' & g_\sigma^-\end{pmatrix}=\frac{1}{m_+m_-}\left[\left(\frac{\gamma_\sigma+f_\sigma}{m_+}-\omega^2\right)\left(\frac{\gamma_\sigma+f_\sigma}{m_-}-\omega^2\right) - \frac{(\gamma_\sigma'-f_\sigma)^2}{m_+m_-}\right]^{-1}\begin{pmatrix}l_\sigma^- & -l_\sigma'\\ -l_\sigma' & l_\sigma^+\end{pmatrix}, \tag{23}$$

is the Green's function of the system in the momentum representation. In accordance with a general property of Green's functions, poles of its matrix elements, $g_\sigma(\omega,\mathbf{k})$, coincide with eigenfrequencies of a pure crystal,

$$g_\parallel(\omega)\propto(\omega^2-\omega_\parallel^2)^{-1}(\omega^2-\Omega_\parallel^2-d^2)^{-1},$$

$$g_\perp(\omega)\propto(\omega^2-\omega_\perp^2)^{-1}(\omega^2-\Omega_+^2)^{-1}(\omega^2-\Omega_-^2)^{-1},$$

as it follows from Eqs. (11), (12).

Solving Eq. (20) with the help of Eqs. (22), (23), one can obtain Fourier amplitudes of the ion displacements, $\mathbf{A}_+(\mathbf{k})$ and $\mathbf{A}_-(\mathbf{k})$, and the displacements themselves:

$$\mathbf{U}_+(\mathbf{r})=\sum_\sigma\int_{(\mathbf{k})}e^{i\mathbf{k}\cdot\mathbf{r}}\,\mathbf{e}_\sigma(\mathbf{k})\otimes\mathbf{e}_\sigma(\mathbf{k})(g_\sigma^+\mathbf{B}_+ + g_\sigma'\mathbf{B}_-,), \tag{24}$$

$$\mathbf{U}_-(\mathbf{r})=\sum_\sigma\int_{(\mathbf{k})}e^{i\mathbf{k}\cdot\mathbf{r}}\,\mathbf{e}_\sigma(\mathbf{k})\otimes\mathbf{e}_\sigma(\mathbf{k})(g_\sigma'\mathbf{B}_+ + g_\sigma^-\mathbf{B}_-,), \tag{24'}$$

where the symbol $\int_{(\mathbf{k})}$ denotes $(1/N)\Sigma_{\mathbf{k}}\approx(a/2\pi)^3\int d\mathbf{k}$, with wave vectors taken from the first Brillouin zone only.

Substitution of $\mathbf{B}_+$ and $\mathbf{B}_-$, given by Eqs. (21,21'), into Eqs. (24) allows one to express all displacements in terms of $\mathbf{U}_+$ and $U_{\mathbf{n}}$ only, and then obtain a closed system of equations for these variables. In the case of an *isotope impurity*, considered earlier in the scalar model of Ref. 7, we set $\delta\beta=0$ and this system of *spectral equations* reads

$$\mathbf{U}_+=\omega^2\delta m\sum_\sigma\int_{(\mathbf{k})}g_\sigma^+\,\mathbf{e}_\sigma(\mathbf{k})\otimes\mathbf{e}_\sigma(\mathbf{k})\mathbf{U}_+. \tag{25}$$

In a cubic crystal, vector $\mathbf{U}_+$ can be arbitrary (Appendix A), whereas frequencies of excitations are defined by the equation:

$$1=\frac{\omega^2\delta m}{3}\int_{(\mathbf{k})}(g_{\parallel}^{+}+2g_{\perp}^{+})=\delta m\,\omega^2 I(\omega^2), \tag{26}$$

which generalizes Eq. (10) obtained in Ref. 7.

All solutions of these equations can be divided into two classes: extended and local states. Since an impurity destroys the translational symmetry of the crystal, any state is now a superposition of all normal modes available in the first Brillouin zone. For extended states, corresponding to scattering states with well-defined wave vectors, frequencies fall into the bands of a pure crystal. Local states, dependent upon the value of the parameter δm in Eq. (26), may arise outside of the bands. From the structure of $g_{\sigma}(\omega,\mathbf{k})$ it might seem that when a frequency is close to a particular band, the modes from it dominate in the corresponding state. However, because contributions of the near and distant bands could be weakened or strengthened by the low or high density of states in them, direct calculations are required here.

As we already mentioned, the function $\Omega_{-}^2(k)$ reaches its maximum value ω_1^2 at $k=k_0$, close to the center of the Brillouin zone. Its expansion around k_0 does not contain a linear term:

$$\Omega_{-}^2(k)=\omega_1^2-\nu^2a^2(k-k_0)^2+\mathcal{O}[a^3(k-k_0)^3]. \tag{27}$$

It immediately shows that the integral in the left-hand side of Eq. (26) diverges at $\omega=\omega_1$ due to a contribution from the lower polaritons branch. Therefore, considering ω in the frequency gap close to its lower boundary we can omit $g_{\parallel}^{+}$ from Eq. (26) and rewrite $\int_{(\mathbf{k})}g_{\perp}^{+}$ using the density of states, $\rho_{-}(\varepsilon)$, in the lower polaritons band:

$$\begin{aligned}I^{+}(\omega^2)&=\int_{(\mathbf{k})}\frac{2g_{\perp}^{+}}{3}\\&=\left(\frac{a}{2\pi}\right)^3\int\frac{2(\omega^2-c^2k^2)(\gamma_{\perp}+f_{\perp}-\omega^2m_{-})d\mathbf{k}}{3m_{+}m_{-}[\omega^2-\omega_{\perp}^2][\omega^2-\Omega_{+}^2][\omega^2-\Omega_{-}^2]}\\&=\frac{2}{3}\int_C\frac{F(k)\rho_{-}(\varepsilon)d\varepsilon}{\omega^2-\varepsilon},\end{aligned} \tag{28}$$

where $F(k)$ denotes all factors of $g_{\perp}^{+}$, other than $(\omega^2-\Omega_{-}^2)^{-1}$ and the last integration is performed on a complex ε plane (Appendix B).

Near the bottom of the polariton band, for small ε, the density of states have the usual Kohn shape, $\rho_{-}(\varepsilon)\propto\sqrt{\varepsilon}$. The asymptote of $\rho_{-}(\varepsilon)$ near the top of the band, for small $z=\omega_1^2-\varepsilon$, can be found with the help of Eq. (27):

$$\begin{aligned}\rho_{-}(\varepsilon)&=\left(\frac{a}{2\pi}\right)^3\int\frac{ds}{|\nabla\Omega_{-}^2(k)|}\\&\approx\left(\frac{a}{2\pi}\right)^2\frac{(k_0+z^{1/2}/a\nu)^2+(k_0-z^{1/2}/a\nu)^2}{\nu z^{1/2}}\\&=\frac{(ak_0)^2}{2\pi^2\nu z^{1/2}},\end{aligned} \tag{29}$$

where all omitted terms are regular at $z=0$.

Since for $\omega\to\omega_1+0$ the divergent part of $I^{+}(\omega^2)$ is provided by a region of small z, in Eq. (28) we can replace the exact density of states with the found asymptote. Considering $\omega^2-\omega_1^2\ll\omega_1^2$ it allows us to calculate the leading part of $I^{+}(\omega^2)$ and transform the spectral equation (26) into the form (Appendix B):

$$\frac{m_{+}}{\delta m}\approx-\frac{2(ak_0)^2\omega_0^2}{3\pi\nu\sqrt{\omega^2-\omega_1^2}}\frac{m_{-}}{M}. \tag{30}$$

Using estimates made in Sec. II and recalling that $a\nu=v_{\perp}'$, we obtain

$$\frac{\delta m}{m}=-\frac{3\pi c v_{\perp}'^2\sqrt{\omega^2-\omega_1^2}}{a^3\omega_0^3 d}. \tag{31}$$

This result recovers Eq. (14) of Ref. 7 obtained in the scalar model and supports the conclusion of the absence of the lower localization threshold for light isotope impurities.

In a general case of *nonisotope* impurity the spectral system is of the 11th rank with 11 variables, $\mathbf{U}_{+}=U_{+}(\mathbf{0})$, $U_{\mathbf{n}}=\mathbf{n}\cdot\mathbf{U}_{-}(\mathbf{n})$. The system can be further simplified with the help of the crystal symmetry. The exact point group of a cubic crystal includes the space inversion. Therefore, all excitations can be classified by their spatial parity.

For the *odd states*, where $\mathbf{U}_{\pm}(-\mathbf{r})=-\mathbf{U}_{\pm}(\mathbf{r})$, one can see that both $\mathbf{U}_{+}$ and $\mathbf{B}_{+}$ are equal to zero and the rank of the spectral system reduces from 11 to 4. Considering the displacements of four negative ions at corners of one face of the bcc-lattice elementary cell (see Fig. 2) as independent variables, from Eqs. (24) we obtain the following system:

$$\sum_{s'=1}^{4}M_{ss'}U_{s'}=-\frac{n^2}{2\delta\beta}U_s, \tag{32}$$

where index s numerates the chosen ions, their radius vectors are denoted as $\mathbf{n}_s$ and $U_s=U_{\mathbf{n}_s}=\mathbf{n}_s\cdot\mathbf{U}_{-}(\mathbf{n}_s)$. The matrix $M_{ss'}$ here is given by the equation

$$\begin{aligned}M_{ss'}=M(\mathbf{n}_s,\mathbf{n}_{s'})=\sum_{\sigma}\int_{(\mathbf{k})}g_{\sigma}^{-}(\mathbf{e}_{\sigma}\cdot\mathbf{n}_s)\\\times(\mathbf{e}_{\sigma}\cdot\mathbf{n}_{s'})\sin(\mathbf{k}\cdot\mathbf{n}_s)\sin(\mathbf{k}\cdot\mathbf{n}_{s'}).\end{aligned} \tag{33}$$

Using transformation properties of the integrand one can show that the matrix $M_{ss'}$ remains invariant, $M(\hat{\mathbf{Q}}\mathbf{n},\hat{\mathbf{Q}}\mathbf{n}')=M(\mathbf{n},\mathbf{n}')$, under any point transformation $\hat{\mathbf{Q}}$. Therefore, the elements of the symmetric matrix $M_{ss'}$ are equal for equivalent pairs of ions: $M_{11}=M_{22}=M_{33}=M_{44}$, then $M_{12}=M_{23}=M_{34}$ and $M_{13}=M_{24}$. After finding eigenvalues of this matrix we obtain three spectral equations:

$$-\frac{n^2}{2\delta\beta}=\mu_0=M_{11}-M_{13}, \tag{34}$$

$$-\frac{n^2}{2\delta\beta}=\mu_{\pm}=M_{11}+M_{11}\pm 2M_{12}. \tag{34'}$$

The structure of the eigenvectors shows that the states corresponding to μ_{+} and μ_{-} represent ''rhombic'' and ''tetragonal'' oscillations localized around the stationary impurity,

whereas, the states corresponding to μ_0 involve both types of deformations of the elementary cell (Appendix C).

Near the lower boundary of the gap the arguments used in evaluation of Eq. (26) are also applicable. Retaining the leading terms in Eq. (33) and using symmetry properties of the arising expressions (Appendix C), we obtain the following expressions:

$$\mu_0 \approx \frac{1}{5}[n^4-(\mathbf{n}_1\cdot\mathbf{n}_3)^2]\int_{(\mathbf{k})} k^2 g_\perp^- , \tag{35}$$

$$\mu_\pm \approx \frac{1}{5}\left\{(\mathbf{n}_1\cdot\mathbf{n}_3)^2+\frac{n^4}{3}\pm 2\left[(\mathbf{n}_1\cdot\mathbf{n}_2)^2-\frac{n^4}{3}\right]\right\}\int_{(\mathbf{k})} k^2 g_\perp^- . \tag{35'}$$

From the geometry of the elementary cell it follows that $(\mathbf{n}_1\cdot\mathbf{n}_2)=-(\mathbf{n}_1\cdot\mathbf{n}_3)=n^2/3=a^2/4$ and, therefore, $\mu_0=\mu_-=(a^4/10)\int_{(\mathbf{k})}k^2 g_\perp^-$. It leads to the unique spectral equation for all ''tetragonal'' modes (Appendix B):

$$\frac{\delta\beta}{\gamma}\approx\frac{15\pi\nu\sqrt{\omega^2-\omega_1^2}}{4(ak_0)^4\omega_0^2}\left(\frac{M}{m_+}\right)^2 . \tag{36}$$

This result shows that the odd local states arise upon an infinitesimally small strengthening of local bonds associated with the impurity, $\delta\beta\geqslant+0$. This effect, similar to the isotope impurity case, is due to a singularity of the density of states in the lower polariton band. Equation (36), compared to Eq. (30), has an additional small factor, $(ak_0)^2$. Therefore, for the same relative deviations, $\delta\beta/\beta$ and $\delta m/m$, the odd states lie much closer to the gap's boundary than the states associated with an isotope impurity. Moreover, these states are much less sensitive to variations of parameters than the isotope-induced local states. This fact reveals itself in an extreme form for ''rhombic'' modes corresponding to μ_+. Equation (35′) gives $\mu_+=0$ which means that within the approximations used these states appear right at the gap's bottom for any value of $\delta\beta$. Accounting for the higher-order terms in expansions of the sin functions in Eq. (31) will separate these modes from the gap's boundary but the separation, $\sqrt{\omega^2-\omega_1^2}\propto\delta\beta(ak_0)^6$, remains the smallest among all considered local states.

For the *even states*, where $\mathbf{U}_\pm(-\mathbf{r})=\mathbf{U}_\pm(\mathbf{r})$, the spectral system contains seven independent variables. Those are components of the impurity displacement $\mathbf{U}_+$ and radial projections of the displacements of four chosen neighboring ions U_s. The elements of the matrix in the corresponding spectral system can be written as integrals of the Green's-function elements, similar to Eq. (33). Considering local states near the gap's bottom, we again can retain in these integrals only transverse terms and use the power expansions of nonsingular factors of the integrands. As it was shown above, $\int_{(\mathbf{k})}(ak)^2 g_\perp^- \ll \int_{(\mathbf{k})} g_\perp^-$ due to the dominant contribution of the small-k region in these integrals. Therefore, since the local states near the gap's bottom are, roughly, ''made'' of long-wavelength polaritons, we can disregard the exponential factors in the matrix elements of the spectral system $[\exp(\pm i\mathbf{k}\cdot\mathbf{n})\approx 1]$ and neglect in Eqs. (21) differences between displacements of identical ions within the elementary cell, $\mathbf{U}_-\approx U_-(\mathbf{n})$. These approximations lead to the following spectral system for even states:

$$\begin{pmatrix}\mathbf{U}_+\\ \mathbf{U}_-\end{pmatrix}\approx\begin{pmatrix}I^+ & I'\\ I' & I^-\end{pmatrix}\begin{pmatrix}\omega^2\delta m-8\delta\beta/3 & 8\delta\beta/3\\ 8\delta\beta/3 & -8\delta\beta/3\end{pmatrix}\begin{pmatrix}\mathbf{U}_+\\ \mathbf{U}_-\end{pmatrix}. \tag{37}$$

The corresponding spectral equation reads

$$\frac{8\delta\beta}{3}(I^++I^--2I')-\omega^2\delta m I^++1 = \frac{8\omega^2\delta\beta\delta m}{3}(I^+I^--I'^2), \tag{38}$$

where all I factors are straightforward to evaluate near the gap's bottom (Appendix B):

$$I^\pm(\omega^2)=\frac{2}{3}\int_{(\mathbf{k})} g_\perp^\pm \approx \frac{2(ak_0)^2}{3\pi\nu\sqrt{\omega^2-\omega_1^2}}\frac{\mu-m_\mp}{m_+m_-}, \tag{39}$$

$$I'(\omega^2)=\frac{2}{3}\int_{(\mathbf{k})} g_\perp' \approx \frac{2(ak_0)^2}{3\pi\nu\sqrt{\omega^2-\omega_1^2}}\frac{\mu}{m_+m_-}. \tag{39'}$$

The right-hand side of Eq. (38) is proportional to a determinant of a degenerate operator, the transverse propagator, and it must be equal to zero identically. Substitution of Eqs. (39), (39′) into Eq. (38) shows this explicitly and transforms the spectral equation of the even states into the following one:

$$\frac{2(ak_0)^2}{3\pi\nu\mu\sqrt{\omega^2-\omega_1^2}}\left[\frac{8\delta\beta}{3}-\omega_0^2\delta m\left(\frac{m_-}{M}\right)^2\right]=1. \tag{40}$$

One can check that here ion displacements satisfy the relationship, $m_-^2\mathbf{U}_+ + m_+^2\mathbf{U}_-=0$, corresponding to optical vibrations.

If we set $\delta\beta=0$ in Eq. (40) it reproduces Eq. (30) obtained earlier for an isotope impurity. That equation has a solution only when $\delta m<0$. In a general case even local states exist only if variations of parameters satisfy the inequality:

$$\delta\beta-\frac{3}{8}\omega_0^2\delta m\left(\frac{m_-}{M}\right)^2>0. \tag{41}$$

Equations (36), (40) allow us to outline regions of the local states (Fig. 3) on a plane of impurity parameters, $\delta m,\delta\beta$. Taking into account obvious physical limitations, $\delta m\geqslant -m_+$, $\delta\beta\geqslant-\beta$, one can see that odd states appear in the right upper quadrant bounded by the lines $\delta m=-m_+$, $\delta\beta=0$. The region of even states is to the right of $\delta m=-m_+$ and above the critical line, $\delta\beta=(3/8)\times(m_-/M)^2\omega_0^2\delta m$. All other areas of $(\delta m,\delta\beta)$ plane are blocked for the polariton localization.

Since we deal with local states near the gap's bottom, our analysis is valid in a vicinity of the critical line for even states, and close to the δm axis for odd states. When the impurity parameters move outside these regions the frequencies of the corresponding local states move away from the gap's bottom. The lines where the frequencies approach the top of the gap establish the outer boundaries of the localization regions. Unlike the situation near the gap's bottom, all terms of all spectral equations remain finite when ω tends to ω_2, which guarantees an existence of limited localization

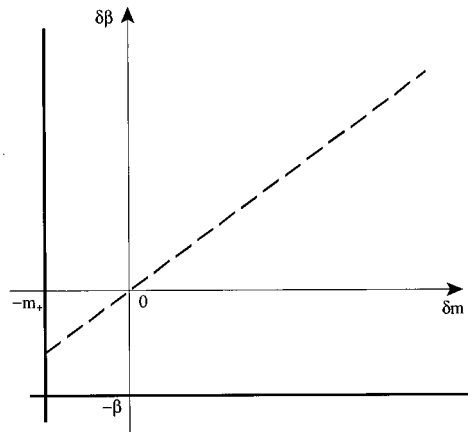

FIG. 3. Regions of existence of local polariton states. δm is the difference between masses of the impurity and a host atom, $\delta\beta$ is the impurity-induced deviation of the elastic constant within the near-neighbor shell, m_+ is the mass of a host ion in the ''positive'' sublattice, β is the elastic constant of a near-neighbor interaction in a perfect crystal. Odd local polariton states exist in the region bound by the solid lines $\delta m=-m_+$, $\delta\beta=0$. The region of even local states is to the right of the solid line $\delta m=-m_+$, and above the dashed line $\delta\beta=(3/8)(m_-/M)^2\omega_0^2\delta m$.

regions. On the other hand, this makes it impossible to do any rigorous analytical calculations. However, using the density-of-states representation of the spectral equations, analogous to Eq. (28), and utilizing some trial functions to simulate densities of states in all bands, one can obtain qualitatively reliable results. Our preliminary estimates show that near the upper boundary of the gap local states are substantially composed of transverse and longitudinal phonons. The balance between them depends on widths of the corresponding bands and the polariton gap. The contribution of the long-wavelength transverse polaritons into these states is proportional to $(v/c)^3$ and is negligible. Roughly, it is caused by the fact that the density of states is inversely proportional to v^3 for phonons and to cv^2 for long-wavelength polaritons. A more detailed analysis of states located far away from the gap's bottom will be presented elsewhere.

IV. DISCUSSION AND CONCLUSIONS

We have considered local polariton states in bcc ionic crystals. It was assumed that the crystal anisotropy is weak and can be neglected in the long-wavelength limit. This approximation was proved to be self-consistent for states located near the bottom of the polariton gap. We found two series of local states, different in parity. The new states appear right at the bottom of the polariton gap upon infinitesimally small variations of an impurity parameters. This is in contrast with 3D phonon systems where a lower threshold for local states always exists.[1,2,9] In Ref. 9 the general theorem regarding the presence of the threshold for arising local states in bandgaps of periodic systems were given. However, the proof assumed the finite values of density of states in the entire band of the pure system. We show that the singularity in the density of states in the lower polariton band causes the absence of this threshold. This singularity also provides that the states near the gap's bottom are formed mostly by long-wavelength transverse polaritons. The local states move toward the upper boundary of the gap upon increase of impurity parameters δm and/or $\delta\beta$.

We have outlined regions of new local polariton states on a plane of impurity parameters. In a region where both types of states coexist, the odd states precede the even ones. They appear first at the gap's bottom and remain near it when the impurity parameters vary much longer than the even states. Local states are a mixture of transverse phonons and photons. Comparing amplitudes of the field E and the crystal polarization P one can make an estimate of the energy partitions of local polariton states. Because the characteristic momentum k_0 happened to be away from the polariton resonance region, the ratio E/P turns out to be of the order of $v'_\perp/c$. An account for the electronic polarization of ions renormalizes c and increases this ratio. A more detailed analysis of these aspects of the polariton local states will be done elsewhere. Condition (41) can help in a search for compounds where local polariton states can be observed.

The results of this paper were obtained within the harmonic approximation of crystal dynamics. Phonon-phonon interaction caused by a lattice anharmonism will affect this picture. Phonon-phonon scattering causes damping of all elementary excitations and the local states as well. It leads to a broadening of all spectral lines and it also washes out all sharp boundaries in the initial excitation spectra. However, it seems physically evident that the scale of this broadening is far below the typical width of phonon bands and cannot change the topology of the initial band structure, or close the polariton gap. If we dress up the elementary excitations and renormalize their spectra, the maximum of the density of states in the lower polariton band and the corresponding singularity will persist after the renormalization since it has a topological origin. That, in turn, guarantees the absence of a threshold for local states near the (renormalized) gap's bottom at zero temperature. However, at nonzero temperature thermal broadening of spectral lines will set a finite threshold for local states.

Another factor that leads to a threshold is crystal anisotropy. It provides a difference between maxima of $\Omega_-^2(\mathbf{k})$ in different directions that causes the density of states in the lower polariton branch to be finite everywhere. It should be emphasized, however, that properties of the local polariton states remain quite different from the corresponding properties of purely phonon local states. Particularly, one can see from our results, that eigenfrequencies of local polaritons are much more sensible to the crystal structure of the host materials.

ACKNOWLEDGMENTS

We wish to thank I.M. Vitebsky for useful discussion. This work was supported by the NSF under Grant No. DMR-9632789, by a CUNY collaborative grant and PSC-CUNY grant.

APPENDIX A

It is known that under any point transformation $\hat{\mathbf{Q}}$ the frequency of any normal mode remains invariant, $\omega^2(\hat{\mathbf{Q}}\mathbf{k})=\omega^2(\mathbf{k})$, and the corresponding polarization vector transforms as follows: $\mathbf{e}(\hat{\mathbf{Q}}\mathbf{k})=\hat{\mathbf{Q}}^{-1}\mathbf{e}(\mathbf{k})$. Because the Brillouin

zone also maps exactly into itself, one can see that

$$\hat{\mathbf{T}}=\int_{(\mathbf{k})} g[\omega^2(\mathbf{k})]\ \mathbf{e}(\mathbf{k})\otimes\mathbf{e}(\mathbf{k})=\int_{(\hat{\mathbf{Q}}\mathbf{k})} g[\omega^2(\hat{\mathbf{Q}}\mathbf{k})]\ \mathbf{e}(\hat{\mathbf{Q}}\mathbf{k}) \otimes\mathbf{e}(\hat{\mathbf{Q}}\mathbf{k})=\hat{\mathbf{Q}}^{-1}\hat{\mathbf{T}}\hat{\mathbf{Q}}. \tag{A1}$$

Therefore, any tensor of this type is an invariant of the point group of a crystal. In the cubic system any group-invariant operator must be trivial, $\hat{\mathbf{T}}=t\ \hat{\mathbf{I}}$, since the group contains a noncollinear axis of different order. Calculating the trace of the operator, one can find

$$\hat{\mathbf{T}}=1/3\int_{(\mathbf{k})} g[\omega^2(\mathbf{k})][\mathbf{e}(\mathbf{k})\cdot\mathbf{e}(\mathbf{k})]\hat{\mathbf{I}}, \tag{A2}$$

where $\hat{\mathbf{I}}$ is the identity operator.

APPENDIX B

The density of states in the lower polariton band $\rho_-(\varepsilon)$ is defined at the complex ε plane, cut from 0 to ω_1^2. The contour of integration C in Eq. (26) runs along the upper side of the cut (it corresponds to integration over $k<k_0$), turns around its right edge and then, for the integration over $k>k_0$, returns along the lower side of the cut to some point $\omega_1'^2$, fixed by the bottom of the optical photon band.

As it was discussed in the text, the leading part of $I(\omega^2)$ at $\Delta(\omega)=\omega^2-\omega_1^2\ll\omega_1^2$, comes from the region close to the right edge of the cut, $\varepsilon=\omega_1^2$. Therefore, evaluating Eq. (26), we can use there the asymptote of the density of states given by Eq. (27). In addition, as it follows from Eq. (25), $k-k_0=\mp z^{1/2}/a\nu$ near the right edge of the cut at its upper and lower sides, respectively. Taking this into account when expanding $F(k)$ around k_0 in Eq. (26), we obtain

$$I^+(\omega^2)=\int_0^{\omega_1^2}\frac{2[F_0-F_0'\sqrt{z}/a\nu+\cdots]dz}{3\sqrt{z}(\Delta+z)}+\int_0^{\omega_1^2-\omega_1'^2}\frac{2[F_0+F_0'\sqrt{z}/a\nu+\cdots]dz}{3\sqrt{z}(\Delta+z)}. \tag{B1}$$

A rescaling $z\to z\Delta$ shows that contributions in $I^+(\omega^2)$ from all terms of expansion of $F(k)$ tend to zero in the limit $\Delta\to+0$, except for the first two terms. Further elementary integration gives the singular part of the considered integral:

$$I^+(\omega^2)=\frac{2(ak_0)^2F(k_0)}{3\pi\nu\Delta^{1/2}}=\frac{2(ak_0)^2}{3\pi\nu\Delta^{1/2}}\frac{(\omega^2-c^2k_0^2)[\gamma_\perp(k_0)+f_\perp(k_0)-m_-\omega^2]}{m_+m_-[\omega^2-\Omega_+^2(k_0)][\omega^2-\omega_\perp^2(k_0)]}. \tag{B2}$$

This result is asymptotically exact since all omitted terms are regular at $\Delta\to+0$. Using estimations made in Sec. II and taking into account conditions $ak_0\ll1$, $v_\perp'^2k_0^2\ll\omega_0^2$, $c^2k_0^2\gg\omega_0^2$, and $\omega\approx\omega_1\approx\omega_0$, it is straightforward to obtain

$$I^+(\omega^2)\approx-\frac{2(ak_0)^2}{3\pi\nu\sqrt{\omega^2-\omega_1^2}}\frac{m_-}{Mm_+}, \tag{B3}$$

which immediately leads to Eq. (28).

In a similar way one can obtain Eqs. (37), as well as, calculate the integral in Eqs. (33):

$$\int_{(\mathbf{k})}(ak)^2g_\perp^-=\frac{2(ak_0)^4}{3\pi\nu\Delta^{1/2}}\frac{(\omega^2-c^2k_0^2)[\gamma_\perp(k_0)+f_\perp(k_0)-m_+\omega^2]}{m_+m_-[\omega^2-\Omega_+^2(k_0)][\omega^2-\omega_\perp^2(k_0)]}\approx-\frac{2(ak_0)^4\omega_0^2}{3\pi\nu\sqrt{\omega^2-\omega_1^2}}\frac{m_+}{Mm_-}. \tag{B4}$$

APPENDIX C

Equation (30) with the matrix $M_{ss'}$ defined by Eq. (31) can be rewritten as follows:

$$\begin{pmatrix} M_{11}-M_{13}-\mu & 0 & 0 & 0\\ 0 & M_{11}-M_{13}-\mu & 0 & 0\\ M_{13} & M_{12} & M_{11}+M_{13}-\mu & 2M_{12}\\ M_{12} & M_{13} & 2M_{12} & M_{11}+M_{13}-\mu \end{pmatrix}\begin{pmatrix} U_1\\ U_2\\ U_3-U_1\\ U_4-U_2\end{pmatrix}=0, \tag{C1}$$

which has three eigenvalues given by Eqs. (32).

For $\mu=\mu_\pm$ this equation gives $U_1=U_2=0$ and $U_3=\pm U_4$. Recalling that $U_s=\mathbf{n}\cdot\mathbf{U}(\mathbf{n}_s)$ and the states we consider here are antisymmetric, one can see that in the μ_+ mode the elementary cell enclosing a defect experiences ''rhombic'' deformations. In the μ_- mode, since the ion motion is antiphased, it produces ''tetragonal'' deformations. For $\mu=\mu_0$ Eq. (C1) leaves U_1 and U_2 independent, whereas, $U_3=U_1/2$ and $U_4=U_2/2$. It results in combined, ''tetrarhombic''deformations of the elementary cell in these modes.

To obtain the explicit expressions of the eigenvalues μ, we have to calculate the matrix elements $M_{ss'}$. When the frequency of the considered states is close to ω_1 we can retain only first terms in expansions of sin factors in Eq. (29). This approximation is self-consistent, because the region of

small wave vectors is the major contribution in Eq. (29). Carrying out the calculations, one needs to know tensors of two types: $\int_{\mathbf{k}} f(k) k^{\alpha} k^{\beta}$ and $\int_{\mathbf{k}} f(k) k^{\alpha} k^{\beta} k^{\sigma} k^{\beta}$, where $f(k)$ is an arbitrary invariant function. From Appendix A it immediately follows that, $\int_{\mathbf{k}} f(k) k^{\alpha} k^{\beta} = (1/3)\delta^{\alpha\beta} \int_{\mathbf{k}} f(k) k^2$. The second tensor is obviously totally symmetric, therefore,

$$\int_{\mathbf{k}} f(k) k^{\alpha} k^{\beta} k^{\sigma} k^{\beta} = I(\delta^{\alpha\beta}\delta^{\sigma\beta} + \delta^{\alpha\sigma}\delta^{\beta\beta} + \delta^{\alpha\beta}\delta^{\beta\sigma}) \int_{\mathbf{k}} f(k) k^4, \tag{C2}$$

where summation over $\alpha = \beta$ and $\sigma = \beta$ defines the numerical factor, $I = 1/15$. Using these results in $M_{ss'}$ and retaining there the transverse terms only, we obtain

$$M_{ss'} \approx \frac{1}{3}\left\{ (\mathbf{n}_s \mathbf{n}_{s'})^2 - \frac{n^4 + 2(\mathbf{n}_s \mathbf{n}_{s'})^2}{5} \right\} \int_{(\mathbf{k})} k^2 g_{\perp}^{-}, \tag{C3}$$

that, in turn, leads to Eqs. (33).

[1] *Lattice Dynamics* (Benjamin, New York, 1969).

[2] A. A. Maradudin, E. W. Montroll, G. H. Weiss, and I. P. Ipatova, *Theory of Lattice Dynamics in the Harmonic Approximation* (Academic, New York, 1971).

[3] I. M. Lifshitz, Dokl. Akad. Nauk SSSR **48**, 83 (1945).

[4] I. M. Lifshitz, Zh. Eksp. Teor. Fiz. **17**, 1017 (1947).

[5] I. M. Lifshitz, Zh. Eksp. Teor. Fiz. **18**, 298 (1948).

[6] M. Born and K. Huang, *Dynamical Theory of Crystal Lattices* (Clarendon, Oxford, 1954).

[7] L. I. Deych and A. A. Lisyansky, Phys. Lett. A (to be published). A. A. Lisyansky and L. I. Deych, Bull. Am. Phys. Soc. **42**, 203 (1997).

[8] C. Kittel, *Introduction to Solid State Physics* (Wiley, New York, 1986).

[9] A. Figotin and A. Klein, J. Stat. Phys. **86**, 165 (1997).